13. H. O. Amman, "Experimental study of the starting process reflection nozzle," Phys. Fluids, 12, No. 5 (1969).

DYNAMICS OF THE CONDENSATION FRONT DURING LASER REDUCTION OF METALS IN HIGH-PRESSURE GASES

A. G. Gnedovets, E. B. Kul'batskii, S. V. Selishchev, A. L. Smirnov, and A. A. Uglov

UDC 536.422.4

Adiabatic expansion of the vapors from a target in a vacuum under the action of laser emission of moderate intensity against solid targets is accompanied by condensation of that vapor into droplets, and here a condensation discontinuity is formed near the surface [1]. As a result of this laser vaporization of the materials in a gaseous medium of elevated pressure (0.1-10 MPa) a condensed phase is also formed [2]. With laser irradiation of the oxides in a reduction gaseous medium we can find conditions under which the condensed phase will consist primarily of metal particles.

The efficiency of the physicochemical processes of laser reduction of oxides in gaseous reduction media of elevated pressure is determined to a considerable extent by the nature of the gasdynamic flows of multiphase vapor-gas mixtures. A study of the dynamics of the multiphase medium near a surface under the action of laser emission (LE) against materials in gases of elevated pressure by a high-speed photographic recording method demonstrated that the nature of the flows depends to a considerable extent on the pressure and kind of gas, the density of the LE flux, etc. [3, 4]. However, the method of high-speed photographic recording does not allow us to study in detail the process involved in the formation of the dispersion phase within the condensation region. We cannot establish the relationship between the space–time characteristics of the condensation region and the pressure of the gas, the energy parameters of the LE, etc. Moreover, it remains unclear as to when condensation begins, i.e., during the time that the LE is directed at the material, or at the conclusion of this stage.

It is demonstrated in this study that a condensation front analogous to this condensation shock arises in the vapor-gas cloud. Double-exposure holographic interferometry was employed to investigate the dynamics of this condensation front while a laser beam was directed against a target in a gas of elevated pressure.

The diagram of the experimental setup is shown in Fig. 1. The radiation from the diagnostic ruby laser 1, on passing through diaphragm 2, is expanded by negative lens 4, is divided into subject and reference rays by means of semitransparent mirror 5, and it is

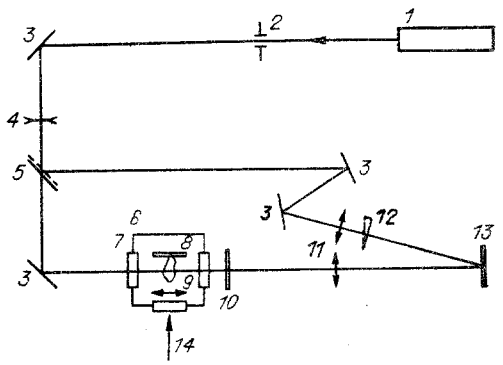

Fig. 1

Moscow. Translated from Zhurnal Prikladnoi Mekhaniki i Tekhnicheskoi Fiziki, No. 4, pp. 38-41, July-August, 1990. Original article submitted February 17, 1989.

0021-8944/90/3104-0540$12.50 © 1991 Plenum Publishing Corporation

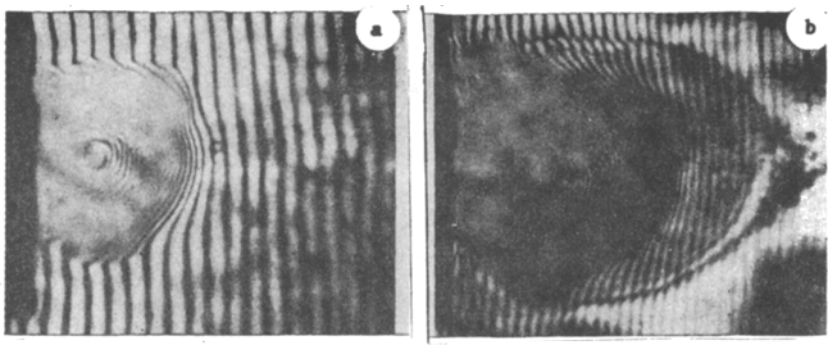

Fig. 2

directed at the photographic plate 13 by means of mirrors 3. The subject beam passes through windows 7 of the high-pressure chamber 6 and probes the vapor-gas cloud 9. The image of the vapor-gas cloud is built up through light filter 10 on the photographic plate by means of objective 11. An objective and a rotating wedge 12 is also placed into the reference beam. The radiation from the neodymium laser pulse (20-50 J, with a duration of 1.5 msec) is focused on target 8 made of tungsten trioxide into a spot with a diameter of 2-6 mm by lens 14 with a focal distance of 270 mm. The intensity of the LE was varied within limits of 10^9-10^{10} W/m^2. The ruby laser emitted pulses in a modulated figure-of-merit regime with an energy of 0.3 J and a duration of 20 nsec. The synchronization circuit provided for the positioning of the diagnostic ruby-laser pulse with an accuracy relative to the neodymium laser pulse of no worse than 5 μsec. With the holographic interferometer we were able to achieve a visualization-field resolution of no less than 50 μm. On completion of the reduction the holographic interferograms were processed numerically. The targets were fabricated in the form of plates with dimensions of 10 × 15 × 1 mm and placed inside the elevated-pressure chamber. The chamber was repeatedly flushed and filled with hydrogen to pressures of 0.1-5.0 MPa. As a result of these experiments we produced a series of holograms which reflect the dynamics of the laser metal reduction process.

Let us highlight some of the main stages in the process of laser metal reduction. The first stage involves the heating of the target and the vaporization of the tungsten trioxide, with formation of the vapor-gas cloud. The reduction of the tungsten trioxide to metallic tungsten occurs primarily in the vapor-gas phase. The second stage involves the formation of the condensation front, while the third stage is relaxation. The first stage lasts approximately 150 μsec. The speed with which the vapors dissipate in this stage depends on the radiation regime and covers a range of $5 \cdot 10^3$-$5 \cdot 10^4$ cm/sec. The second stage begins 1500 μsec after completion of the LE pulse. Relaxation takes up yet another 2-3 μsec. A unique feature of the process of laser vaporization of materials in high-pressure gases is the change in the nature of the target-vapor flows in the manner in which they are dependent on pressure. Thus, for example, for an ambient-gas pressure less than or equal to 1 MPa we observe that the vapors from the target flow in the manner of a jet. As the pressure is increased, the mechanism of vapor dissipation undergoes a change and for pressures higher than 1 MPa the vapors are propagated by diffusion.

Interferograms of the laser reduction process are represented in Fig. 2. In the interferogram shown in Fig. 2a, corresponding to the instant of time 150 μsec, the target vapor cloud has been visualized. The characteristic position of the condensation front is shown in the interferogram in Fig. 2b. In all of these interferograms the region occupied by the vapor-gas phase is distinguished by an increase in the refraction index relative to the free visualization field, which is primarily associated with the increase in the concentration of tungsten atoms. A reduction in the refraction index in the region occupied by the vapor-gas phase behind the condensation front (Fig. 2b) may come about as a result of the reduction in the density of the vapor-gas mixture as a consequence of the formation of a shock wave, as a result of vapor condensation, or because of the presence of an electron component whose contribution to the change in the refractive index is negative, i.e., the increase in electron concentration leads to a reduction in the refractive index. The latter may be a consequence of all of these factors.

We should take note of the fact that no shock or sound waves were visualized on the holograms. Moreover, the direction of the motion of the front coincides with the direction

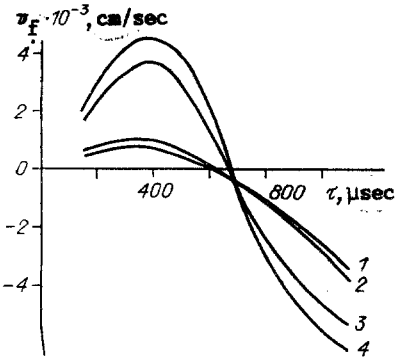

Fig. 3

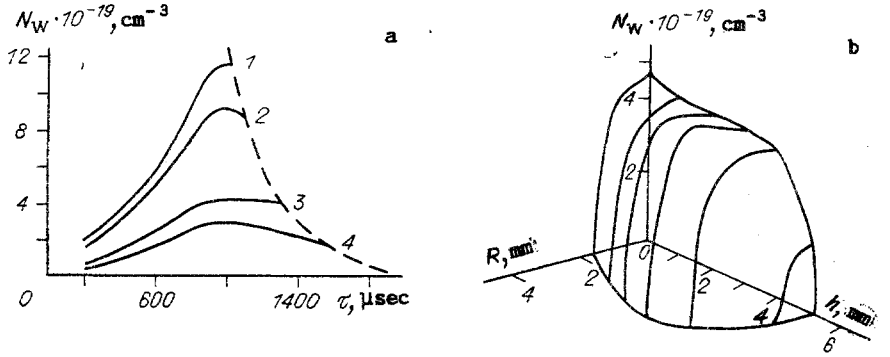

Fig. 4

of the temperature-field gradient in the vapor-gas phase. It thus made it possible to establish that the front which we observed was in fact the condensation front.

The condensation front arises at the periphery of the vapor-gas cloud, where the vapor-gas phase is cooled and supersaturated. Its motion at $p \leq 1$ MPa, i.e., in the case of a vapor jet, differs from the motion at $p > 1$ MPa in the case of diffusion. The main feature lies in the fact that with a vapor jet the condensation front, perpendicular to the LE axis, exhibits no clear outlines. In this case, it is clearly defined only at the boundary of the vapor-gas cloud, positioned parallel to the axis of the LE. The condensation front in the case of diffusion for the vapors of the target during the early moments replicate the outlines of the boundaries of the vapor-gas cloud, straightening out by the end of the LE. Thus, with $p \leq 1$ MPa the condensation front moves along the radius in the direction from the axis of the vapor-gas cloud as the cloud expands during the first 600-700 μsec, and then it moves toward the axis of the vapor-gas cloud, as the rate of cloud expansion lessens to ~10^2 cm/sec. With $p > 1$ MPa the condensation front initially moves in a direction away from the target, for so long as the rate of disintegration for the vapor-gas cloud increases and does not equal the velocity of the condensation front. Then it changes direction in a complete reversal and begins to move toward the surface of the target. The velocity of the front increases to $12 \cdot 10^3$ cm/sec. The change in the velocity of the condensation front, measured relative to the LE axis (1, 2: 0.1 and 0.5 MPa) and relative to the target surface (3, 4: 4 and 5 MPa), is shown in Fig. 3 as a function of time. The change in the sign of the velocity sets in at the instant of time 600-700 μsec. On completion of the LE (1500 μsec) the velocity of the condensation front increases to values greater than $20 \cdot 10^4$ cm/sec within a period of time smaller than 5 μsec ($p > 1$ MPa). With $p \leq 1$ MPa and a jetlike vapor flow we were unable to estimate the velocity of the condensation front subsequent to the completion of the LE, since the vapor-gas phase free of the condensate condenses so rapidly that it was impossible, with sufficient reliability, to resolve the instant of time at which the vapor-gas region implodes. The condensation process subsequent to the completion of the LE in this range of pressures does not exceed 2-5 μsec. Less than 30% (by volume) of the condensate is formed within this time. The change in the concentration of tungsten atoms in the vapor-gas phase (a) and the distribution of the tungsten atom in the vapor-gas phase for $p = 4$ MPa is shown in Fig. 4 in five sections of the target surface (b). The

dashed line in Fig. 4a denotes the position of the condensation front in its dependence on the time and pressure of the gas, the concentration of the tungsten atoms behind the condensation front on the basis of estimates, being reduced by factors of 20-40. The curves correspond to pressures of 0.1, 0.5, 4, and 5 MPa. The concentration of tungsten atoms has been calculated at a point some 2 mm from the surface of the target along the LE axis. Selection of coordinates is governed by convenience of processing the holographic interferograms. In calculating the profiles (Fig. 4b) we assumed that the vapor-gas cloud exhibits axial symmetry and that the LE in this case is directed along the OY axis.

Thus, holographic interferometry of laser reduction of tungsten trioxide in hydrogen demonstrated that the condensation process in its qualitative aspects retains the fundamental physicochemical relationships applicable to condensation in laser vaporization of material under normal conditions or in a rather rarefied atmosphere. Thus, the visualized condensation front is analogous to a jump in condensation [1], such as arises in laser vaporization in a vacuum. A unique feature of laser metal reduction in a high-pressure reducing atmosphere shows up in the fact that when $p \leq 1$ MPa we observe the jetlike flow of the vapors and the condensation front is not clearly defined, and with $p > 1$ MPa the vapors are propagated by diffusion, the condensation front is clearly outlined, and its direction of motion corresponds with that of the temperature-field gradient.

LITERATURE CITED

1. S. I. Anisimov, Ya. A. Imas, G. S. Romanov, and Yu. V. Khodyko, The Effect of High-Power Radiation on Metal [in Russian], Nauka, Moscow (1970).
2. A. A. Uglov, A. G. Gnedovets, and E. B. Kul'batskii, "Heavy-vapor condensation on particles in a light-gas atmosphere," Fiz. Khim. Obrab. Mater., No. 4 (1985).
3. E. B. Kul'batskii and S. V. Selishchev, "The effect of the angle of beam incident on the action of a surface laser plasma on graphite," Fiz. Khim. Obrab. Mater., No. 5 (1987).
4. S. S. Pyrakhin, A. A. Royanov, and S. V. Selishchev, "The dynamics of a surface laser plasma in high-pressure gases," Fiz. Khim. Obrab. Mater., No. 4 (1987).